UCRL-CONF-227196

LAWRENCE LIVERMORE NATIONAL LABORATORY

Assessment of gradient-diffusion closures for modeling Rayleigh-Taylor and Richtmyer-Meshkov instability-induced mixing

O. Schilling, N. Mueschke, M. Latini

January 11, 2007

International Workshop on the Physics of Compressible Turbulent Mixing
Paris, France
July 17, 2006 through July 20, 2006

Disclaimer

e-mail: schilling1@llnl.gov

Assessment of gradient-diffusion closures for modeling Rayleigh–Taylor and Richtmyer–Meshkov instability-induced mixing

Oleg SCHILLING[1], Nicholas MUESCHKE[2] and Marco LATINI[3]

[1] *University of California, Lawrence Livermore National Laboratory, Livermore, California 94551, USA*
[2] *Texas A&M University, College Station, Texas 77843, USA*
[3] *California Institute of Technology, Pasadena, California 91125, USA*

Abstract: The validity of gradient-diffusion closures for modeling turbulent transport in multi-mode Rayleigh–Taylor and reshocked Richtmyer–Meshkov instability-induced mixing is investigated using data from three-dimensional spectral/tenth-order compact difference and ninth-order weighted essentially non-oscillatory simulations, respectively. Details on the numerical methods, initial and boundary conditions, and validation of the results are discussed elsewhere [2, 3]. First, mean and fluctuating fields are constructed using spatial averaging in the two periodic flow directions. Then, quantities entering eddy viscosity-type gradient-diffusion closures, such as the turbulent kinetic energy and its dissipation rate (or turbulent frequency), and the turbulent viscosity are constructed. The magnitudes of the terms in the turbulent kinetic energy transport equation are examined to identify the dominant processes. It is shown that the buoyancy (or shock) production term is the dominant term in the transport equation, and that the shear production term is relatively small for both the Rayleigh–Taylor and Richtmyer–Meshkov cases. Finally, *a priori* tests of gradient-diffusion closures of the unclosed terms in the turbulent kinetic energy transport equation are performed by comparing the terms constructed directly using the data to the modeled term. A simple method for estimating the turbulent Schmidt numbers appearing in the closures is proposed. Using these turbulent Schmidt numbers, it is shown that both the shape and magnitude of the profiles of the dominant terms in the turbulent kinetic energy transport equation across the mixing layer are generally well captured.

1 INTRODUCTION

The purpose of this work is to investigate the mechanisms and modeling of turbulent transport in multi-mode Rayleigh–Taylor and reshocked Richtmyer–Meshkov instability-induced mixing using three-dimensional high-resolution numerical simulation data. The equations solved and the numerical methods used are summarized elsewhere [2, 3]. Using the numerical simulation data validated by comparing to available experimental data, Favre-averaged quantities used in turbulence models closed using the gradient-diffusion approximation are computed from the simulation data. The budget of the terms in the turbulent kinetic energy transport equation is investigated to determine which physical processes are most important to model. Finally, the unclosed terms in the turbulent kinetic energy transport equation are modeled using standard gradient-diffusion (eddy viscosity) closure models and are compared to the same terms computed directly from the simulation data.

2 DEFINITIONS OF AVERAGES AND THE EXACT TURBULENT KINETIC ENERGY TRANSPORT EQUATION

As only one realization each of the Rayleigh–Taylor and Richtmyer–Meshkov unstable flows is considered, ensemble averaging is approximated here by spatial averaging over the two periodic (homogeneous) directions in the simulations: the directions perpendicular to gravity and the directions perpendicular to the shock propagation. The Reynolds and Favre average of a field $\phi(\mathbf{x}, t)$ are taken as

$$\overline{\phi}(z,t) = \frac{1}{L_x\, L_y} \int_0^{L_y}\!\! \int_0^{L_x} \phi(\mathbf{x},t)\, \mathrm{d}x\, \mathrm{d}y \;\; , \;\; \widetilde{\phi}(z,t) = \frac{\overline{\rho\, \phi}}{\overline{\rho}} \tag{2.1}$$

with corresponding fluctuations

$$\phi(\mathbf{x},t)' = \phi(\mathbf{x},t) - \overline{\phi}(z,t) \;\; , \;\; \phi(\mathbf{x},t)'' = \phi(\mathbf{x},t) - \widetilde{\phi}(z,t)\,. \tag{2.2}$$

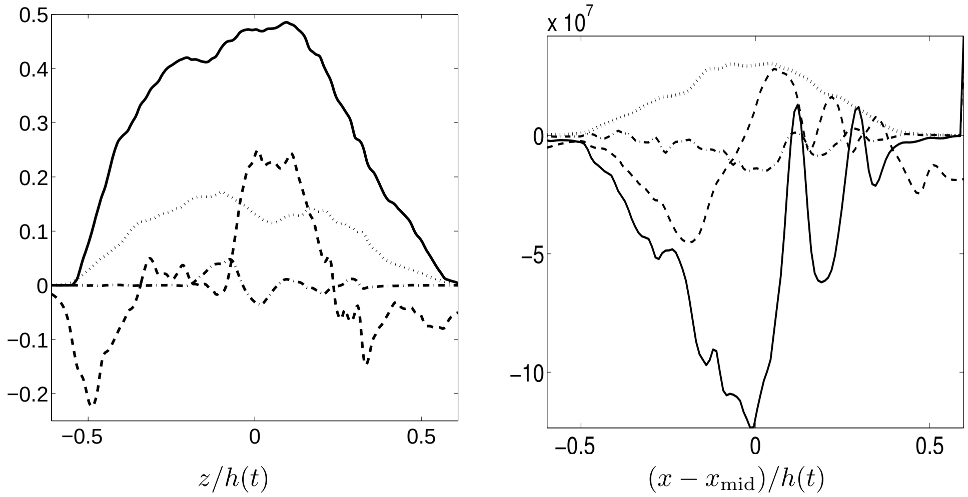

Fig. 3.1. The budget of the terms in the turbulent kinetic energy equation at $\tau = 1$ for the Rayleigh–Taylor flow (left) and at 5 ms for the reshocked Richtmyer–Meshkov flow (right). The buoyancy (shock) production term P_b, the shear production term P_s, the turbulent diffusion term T, and the turbulent kinetic energy dissipation term D are shown using a solid, dash-dot, dashed, and dotted line, respectively.

Here, L_x and L_y are the lengths of the domain in the periodic directions.

The exact, unclosed turbulent kinetic energy ($\widetilde{E''} = \widetilde{u''^2}/2$) transport equation is

$$\overline{\rho}\,\frac{\mathrm{d}\widetilde{E''}}{\mathrm{d}t} = P_b + P_s + T + D + \Pi\,, \tag{2.3}$$

where $\mathrm{d}/\mathrm{d}t = \partial/\partial t + \widetilde{u}_j \partial/\partial x_j$ and the buoyancy (or shock) production, shear production, turbulent diffusion, turbulent dissipation, and pressure-dilatation terms are

$$P_b \equiv -\overline{u''_j}\left(\frac{\partial \overline{p}}{\partial x_j} - \frac{\partial \widetilde{\sigma}_{ij}}{\partial x_i}\right) \;,\; P_s \equiv -\overline{\rho\, u''_i\, u''_j}\,\frac{\partial \widetilde{u}_i}{\partial x_j} \;,\; T \equiv -\frac{\partial}{\partial x_j}\left(\overline{\rho\, E''\, u''_j} + \overline{p'\, u''_j} - \overline{u''_i\, \sigma''_{ij}}\right), \tag{2.4}$$

$$D \equiv -\overline{\sigma''_{ij}\,\frac{\partial u''_i}{\partial x_j}} \;,\; \Pi \equiv \overline{p'\,\frac{\partial u''_j}{\partial x_j}}\,,$$

respectively. In the shock-capturing simulation of the Richtmyer–Meshkov instability, viscous terms are not explicitly included, so that $\widetilde{\sigma}_{ij} = \sigma''_{ij} = 0$ formally in P_b and T. The terms involving $\widetilde{\sigma}_{ij}$ and σ''_{ij} are also very small in the Rayleigh–Taylor simulation (except in D), and are not considered further. The turbulent dissipation D is computed explicitly in the Rayleigh–Taylor case, but can only be modeled in the Richtmyer–Meshkov case.

3 TIME-EVOLUTION OF TERMS IN THE EXACT TURBULENT KINETIC ENERGY TRANSPORT EQUATION

The time-evolution of terms in the exact turbulent kinetic energy transport equation is considered here for both the Rayleigh–Taylor and Richtmyer–Meshkov flow cases to determine which terms are dominant in these instabilities. For each term, the profile across the mixing layer is shown, *i.e.*, the term in (2.3) integrated over the periodic directions using the Favre and Reynolds average definitions. The coordinate in the direction of gravity or the shock is scaled by the mixing layer width $h(t)$. In addition, in the Richtmyer–Meshkov flow case, the coordinate is recentered by the midpoint, x_{mid}, between the bubble and spike fronts.

3.1 Rayleigh–Taylor Unstable Flow

The budget of terms in the turbulent kinetic energy transport equation (2.3) across the mixing layer is shown in Fig. 3.1 at time $\tau = 1$, where $\tau = t/\sqrt{gAH}$ (see [3] for further details of the simulation). It is evident that the buoyancy production term is dominant, with additional significant contributions from the turbulent diffusion and dissipation terms. The shear production term is nearly zero, as expected in a flow with either a nearly constant mean velocity or zero mean velocity. The turbulent diffusion is both positive and negative over the layer, with zero integral, indicating that this term redistributes turbulent kinetic energy conservatively within the layer. The buoyancy production and dissipation terms are positive everywhere, and are peaked near the centerplane of the layer, $z = 0$. The relative importance of these terms and the trends are also true for earlier times (not shown here).

3.2 Richtmyer–Meshkov Unstable Flow

The budget of terms in the turbulent kinetic energy transport equation (2.3) across the mixing layer is shown in Fig. 3.1 at 5 ms (see [2] for further details of the simulation). In the absence of explicit molecular dissipation, the dissipation term is modeled as in the $\widetilde{E''}$-$\widetilde{\omega''}$ model [4]

$$D = -\overline{\rho}\, \widetilde{E''}\, \widetilde{\omega''} \,, \tag{3.1}$$

where $\widetilde{\omega''} = \sqrt{2\widetilde{\Omega''}}$ is the turbulent frequency. The shock production term dominates the other terms, and has largest (negative) value near the centerplane of the mixing layer. As in the Rayleigh–Taylor case, the turbulent diffusion and dissipation terms also contribute significantly. The shear production is oscillatory and averages to nearly zero, as expected in a flow with a nearly constant mean velocity. The turbulent diffusion is both positive and negative over the layer, with zero integral, indicating that this term redistributes turbulent kinetic energy conservatively within the layer. The dissipation term is positive everywhere, and is peaked near the centerplane of the layer.

4 A PRIORI ANALYSIS OF THE GRADIENT-DIFFUSION APPROXIMATION

In the *a priori* analysis of the gradient-diffusion (eddy viscosity) approximation for closing the terms in the exact turbulent kinetic energy transport equation, the profiles of the closed terms across the mixing layer are computed using the models presented below. Modeled terms were constructed from the appropriately averaged simulation data. The model predictions and the directly computed (unclosed) terms are compared to evaluate the predictive capability of the gradient-diffusion closures of the key terms in the turbulent kinetic energy equation.

4.1 The Modeled Turbulent Kinetic Energy Transport Equation

Using the gradient-diffusion hypothesis, the modeled terms (2.4) are given by the algebraic closures [1]

$$P_b = -\frac{\nu_t}{\sigma_\rho\, \overline{\rho}}\, \frac{\partial \overline{\rho}}{\partial x_j}\, \frac{\partial \overline{p}}{\partial x_j} \,, \tag{4.1}$$

$$P_s = -\left[\frac{2}{3}\, \overline{\rho}\, \widetilde{E''}\, \delta_{ij} - 2\, \mu_t \left(\widetilde{S}_{ij} - \frac{\delta_{ij}}{3}\, \frac{\partial \widetilde{u}_k}{\partial x_k}\right)\right] \frac{\partial \widetilde{u}_i}{\partial x_j} \,, \tag{4.2}$$

$$T = \frac{\partial}{\partial x_j}\left(\frac{\mu_t}{\sigma_k}\, \frac{\partial \widetilde{E''}}{\partial x_j}\right), \tag{4.3}$$

$$D = -\overline{\rho}\, \widetilde{\epsilon''} \,, \tag{4.4}$$

where $\widetilde{S}_{ij} = (1/2)(\partial \widetilde{u}_i/\partial x_j + \partial \widetilde{u}_j/\partial x_i)$ is the mean strain-rate tensor, $\widetilde{\epsilon''}$ is the turbulent kinetic energy dissipation rate per unit mass, the pressure-dilatation term Π and the pressure-flux $\overline{p' u''_j}$ contribution to T are neglected in the current study, and σ_ρ and σ_k are dimensionless turbulent Schmidt numbers. With the definitions of the Favre and Reynolds averages, these terms are profiles across the mixing layer depending only on the coordinate in the inhomogeneous direction and on time. In the above expressions,

$$\nu_t = \begin{cases} 0.09\, \dfrac{\left(\widetilde{E''}\right)^2}{\widetilde{\epsilon''}} & \text{for Rayleigh–Taylor flow} \\ \dfrac{\widetilde{E''}}{\widetilde{\omega''}} & \text{for Richtmyer–Meshkov flow} \end{cases} \tag{4.5}$$

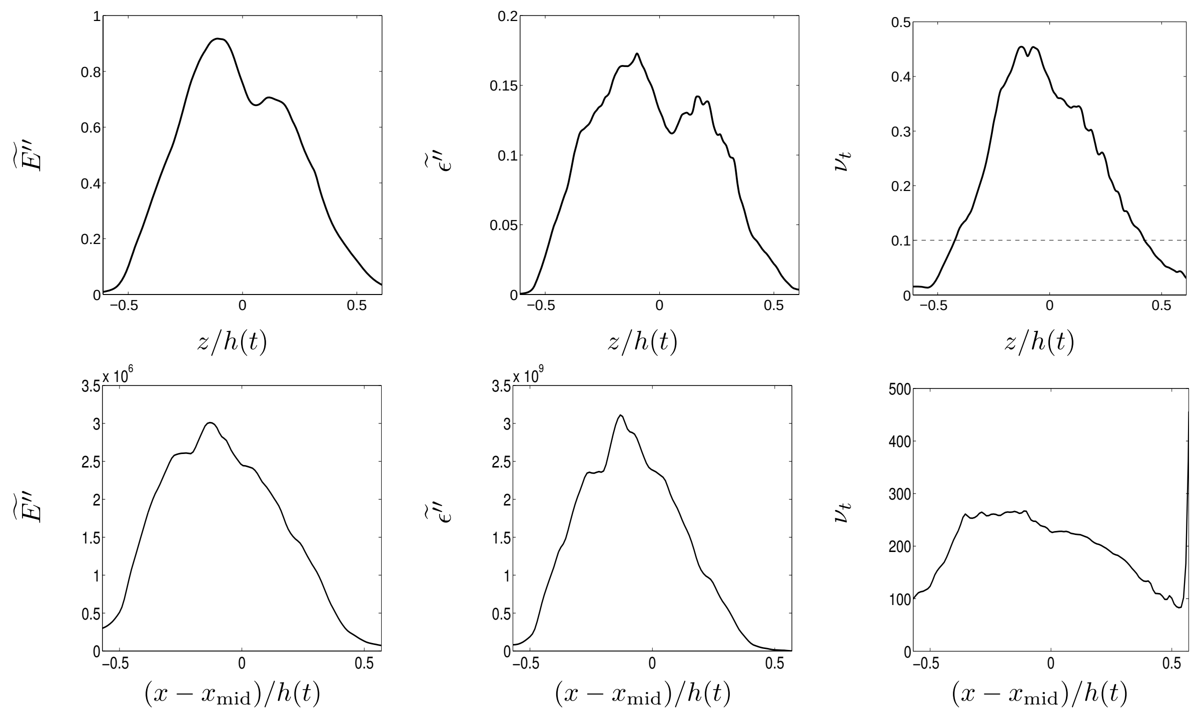

Fig. 4.2. The turbulent kinetic energy $\widetilde{E''}$, turbulent kinetic energy dissipation rate $\widetilde{\epsilon''}$, and turbulent viscosity ν_t at $\tau = 1$ and 5 ms for the Rayleigh–Taylor (top) and Richtmyer–Meshkov (bottom) flows, respectively.

is the turbulent viscosity ($\mu_t = \overline{\rho}\nu_t$).

The turbulent kinetic energy, turbulent kinetic energy dissipation rate, and turbulent viscosity profiles across the mixing layer are shown for the Rayleigh–Taylor and Richtmyer–Meshkov flows in Fig. 4.2. For the Rayleigh–Taylor case, all three quantities are peaked near the center of the mixing layer. Note that the turbulent viscosity is considerably larger than the molecular viscosity $\nu \approx 0.1$ cm^2/s. In order to obtain better correlation between the modeled and directly computed term, the time-dependent turbulent Schmidt numbers were first calculated by algebraically solving for them in Eqs. (4.1) and (4.3) and integrating over the layer for both the Rayleigh–Taylor and Richtmyer–Meshkov flows. The resulting time-dependent values of σ_ρ and σ_k were then used in the closures. Note that this rescaling of the terms does not change their shape, but only adjusts their magnitude.

4.2 Rayleigh–Taylor unstable flow

In the Rayleigh–Taylor instability, it was found that σ_ρ approaches a value of ~ 0.1, while σ_k approaches unity at the latest time in the simulation. The profiles are shown as a function of $z/h(t)$, where z is the coordinate direction parallel to gravity and $h(t)$ is the mixing layer width. Thus, the mixing layer is contained within $z/h(t) \in [-0.5, 0.5]$. As seen in Fig. 4.3, the overall agreement between the model and DNS data for $\overline{w''}$ is good. In particular, the shape and magnitude are generally well captured. However, the figure shows that the gradient-diffusion approximation does not completely capture the energy transfer across the layer. The large amplitude excursions in the model are a consequence of the poor statistical convergence of the mean density and turbulent kinetic energy gradients due to the limited spatial resolution of the data.

4.3 Richtmyer–Meshkov unstable flow

In the Richtmyer–Meshkov instability, it was found that σ_ρ and σ_k both approach an asymptotic value of ~ 0.1 in the simulation. The profiles are shown as a function of $(x - x_{mid})/h(t)$, where x is the coordinate direction parallel to the shock propagation, x_{mid} is the midpoint of the layer, and $h(t)$ is the mixing layer width. Thus, the mixing layer is contained within $(x - x_{mid})/h(t) \in [-0.5, 0.5]$. As shown in Fig. 4.3, the Reynolds-averaged Favre fluctuating velocity $\overline{u''}$ is in good agreement with the model up to the interaction of

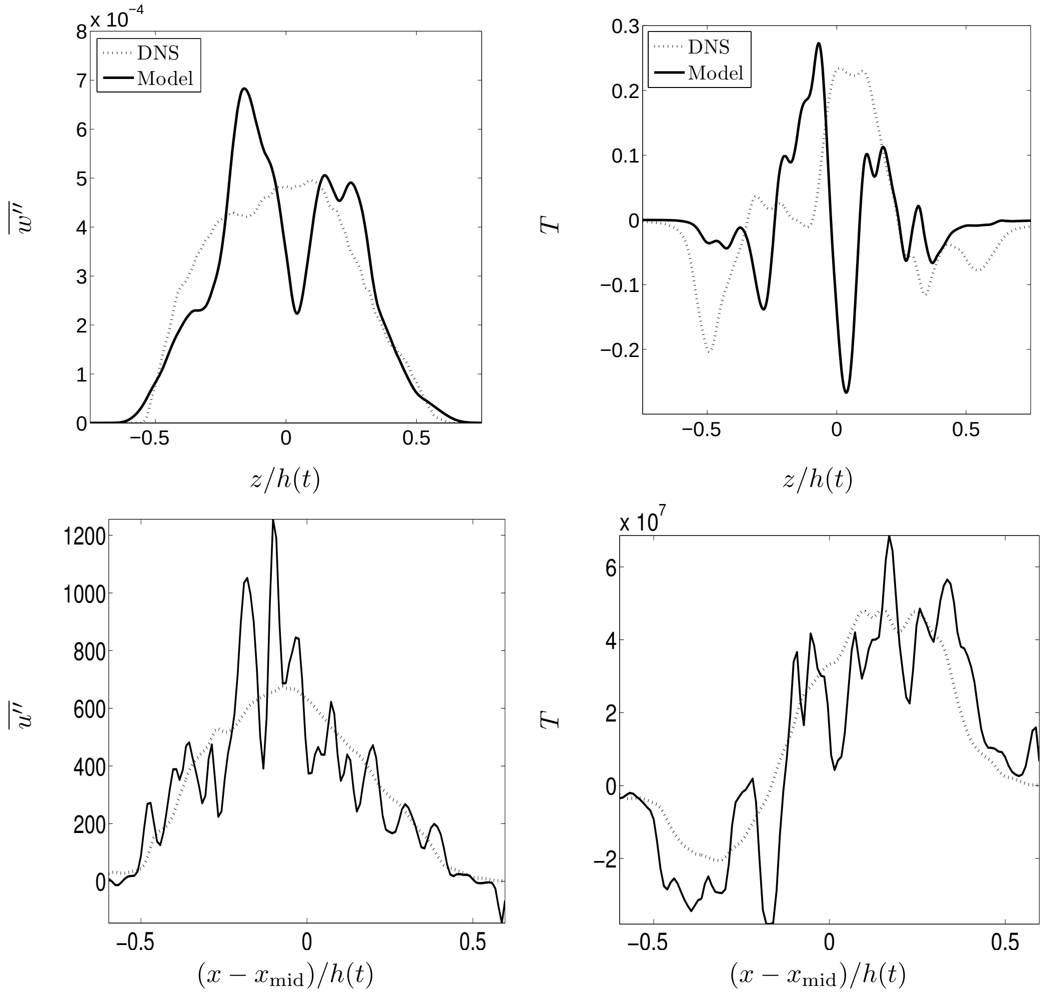

Fig. 4.3. Comparison of the computed and modeled averaged Favre fluctuating velocity and turbulent diffusion, T, for the Rayleigh–Taylor (top) and Richtmyer–Meshkov (bottom) flows.

the layer with the reflected rarefaction at ~ 5 ms. The turbulent kinetic energy diffusion shown in Fig. 4.3 is also in good agreement with the model up to the interaction with the reflected rarefaction. Both quantities exhibit large amplitude excursions in the model due to the poor statistical convergence of the mean density and turbulent kinetic energy gradients.

5 CONCLUSIONS

Using spatially-averaged data from numerical simulation models of the Texas A&M University water channel Rayleigh–Taylor experiment [3] and the reshocked $Ma = 1.5$ air/SF_6 Vetter–Sturtevant Richtmyer–Meshkov instability experiment [2], it was shown that: (1) the buoyancy (shock) production, turbulent dissipation, and turbulent diffusion terms are dominant, while the shear production term is nearly zero in Rayleigh–Taylor flow and less important than the other terms in the Richtmyer–Meshkov flow; (2) using spatial averaging to define Favre and Reynolds averaged and fluctuating fields, it is possible to compute quantities (such as the turbulent viscosity) entering into gradient-diffusion turbulence closures, and; (3) using adjusted values of the turbulent Schmidt numbers (smaller than typically used in compressible and stratified turbulent flow modeling), the gradient-diffusion models for the key terms in the turbulent kinetic energy transport equation are in reasonable qualitative and quantitative agreement with the data in *a priori* comparisons. While the gradient-diffusion approximation cannot correctly capture the anisotropy of the Reynolds stress tensor components in these flows, this approximation is evidently quite reasonable for most of the important terms in the turbulent kinetic energy balance. The only term in the turbulent kinetic energy equation that requires the Reynolds stress tensor is the shear production (4.2): this term is generally of little importance in the overall energy balance in both Rayleigh–Taylor and Richtmyer–Meshkov instability-induced turbulence.

This investigation demonstrates that high-resolution simulations can be used to provide essential data concerning turbulent transport and mixing processes in three-dimensional Rayleigh–Taylor and reshocked Richtmyer–Meshkov instability. In particular, simulations provide quantities not presently possible (or difficult) to measure experimentally, such as the turbulent Schmidt numbers.

Nicholas Mueschke acknowledges support by the National Nuclear Security Administration under the Stewardship Science Academic Alliances program through DOE Research Grant #DE-FG03-02NA00060. This work was also performed under the auspices of the U.S. Department of Energy by the University of California Lawrence Livermore National Laboratory under contract No. W-7405-Eng-48.

REFERENCES

[1] Chassaing, P., Antonia, R. A., Anselmet, F., Joly, L. and Sarkar, S., 2002. *Variable Density Fluid Turbulence*, Fluid Mechanics and its Applications Vol. 69, Kluwer Academic.

[2] Latini, M., Schilling, O. and Don, W. S., 2006. Richtmyer–Meshkov Instability-Induced Mixing: Initial Conditions Modeling, Three-Dimensional Simulations and Comparisons with Experiment, in *Proceedings of the Tenth International Workshop on the Physics of Compressible Turbulent Mixing*, 17–21 July 2006, Paris, France, edited by M. Legrand and M. Vandenboomgaerde.

[3] Mueschke, N., Schilling, O. and Andrews, M. J., 2006. Rayleigh–Taylor Instability-Induced Mixing: Initial Conditions Modeling, Three-Dimensional Simulations and Comparisons with Experiment, in *Proceedings of the Tenth International Workshop on the Physics of Compressible Turbulent Mixing*, 17–21 July 2006, Paris, France, edited by M. Legrand and M. Vandenboomgaerde.

[4] Wilcox, D. C., 2006. *Turbulence Modeling for CFD*, third edition, DCW Industries.